EGS4 Studies of CDF Preshower Response:

B-Field Effects and "Massless Gap" Resolution Response

A. B. Wicklund
High Energy Physics Division, Argonne National Laboratory

January 2, 1992

We have carried out a simplified EGS4 simulation of the response of the central preshower detector ("CPR") in CDF. Test beam results show that the CPR pulse height provides a ~ 95% separation of electrons and pions, with the nominal 1.1 X0 preradiator provided by the magnet coil. Test beam data also suggest that the CPR pulse height could be used to improve the CEM energy resolution, since the CPR response is correlated with energy loss fluctuations in the coil-preradiator. The main purpose of the EGS simulation described in this note is to determine whether the CPR response will be degraded by magnetic field effects. Specifically, the robust electron response of the CPR is obviously due to production of low energy e± secondaries early in the electron shower; we might expect these secondaries to curl up in the magnetic field, leading to a reduced CPR response as compared with the test beam results.

This note summarizes two results from the EGS4 simulation. First, we examine the dependence of the CPR response on B-field, and we find no indication of degradation in CPR pulse height for a 1.5 T field. Second, we examine the possible improvement of the CEM resolution, using the CPR-CEM pulse height correlation (usually referred to as the "massless gap" technique in liquid argon circles). Here we find that only marginal resolution improvements can be expected in the CDF detector, and these improvements are independent of B-field. For a detector with more preradiator material, specifically the SDC detector at larger rapidities, the "massless gap" correction can be used to partially offset the degradation caused by the coil material.

1) EGS4 Description

To approximate the radiator configuration in the outer CTC and CDT, and the coil and cryostat, we used the following layout of absorber materials:

Radius	X0	B-Field	Title
25 cm	0.046	0.0	Outer VTPC/Inner CTC
81	0.000	0.0	"Vac. 0"
138.0 - 141.9	0.3376	"B"	CTC/CDT/Inner Vac. Wall
141.9 - 150.0	0.000	"B"	"Vac. 1"
150.0 - 152.8	0.3151	"B"	Coil (2 cm Al-Cu-NbTi)
152.8 - 159.4	0.000	0.0	"Vac. 2"
159.4 - 163.4	0.4501	0.0	Outer Support, Shield, Vac. Shell
163.4	0.000	0.0	"Vac. 3" (CPR)

In CDF the actual CPR depth is around 170 cm, but in view of the results of this simulation, more precise EGS descriptions are unnecessary. The B-field is turned on only in the regions marked "B" (e.g. 1.5 T in CDF), and the expected shower location at CPR is calculated based on a straight through electron of nominal incident energy. Secondary electrons and photons are sampled in the four "vacuum" regions, (Vac. 0 ..Vac. 3, where Vac. 3 is the CPR plane). "Vac. 3" is chosen to be a 1 cm air gap, to allow measurement of dE/dx for secondary electrons. All non-vacuum regions are taken to be aluminum radiators. The total radiator is 1.1 X0 in the CTC-CDT-coil-cryostat system, of which 0.65 X0 are in the non-zero B-field region. For simplicity, the B-field is constant in the "coil" (as opposed to actual linear falloff); this tends to overestimate the B-field effects, which turn out to be negligible anyway.

In EGS4, we used HOWFAR to propagate electrons and positrons along helical trajectories in the non-zero B-field regions. The typical integration step size in these regions (~ 1 cm) was much smaller than the radius of curvature (e.g. 22 cm for 100 MeV e ± at B = 1.5 T) for energies and B-field values of interest. We note that, while very low energy electrons do curl up in the magnetic field, electrons below around 40 MeV (< 9 cm radius of curvature at 1.5 T) that are produced in the coil region, range out in the aluminum material before reaching the CPR. Thus, in general the B-field mainly affects very low energy electrons that do not contribute to the CPR pulse height. In the EGS4 simulation we explicitly flagged for removal any e ± secondaries that (a) had dR/ds < 0 along the integration step, where R = outward radial direction, or (b) were more than ± 9 cm from the expected electron trajectory at the CPR. We find that at any given layer in the EGS4 setup, the total number of e ± secondaries is roughly independent of B-field, but the fraction of these that are flagged for removal increases linearly with B, as expected.

2) CPR Response as a Function of B-Field

Figures 1 and 2 illustrate the qualitative features of shower development in the 1.1 X0 radiator setup. Figure (1) shows the energy distributions of e ± secondaries in each of the four vacuum regions. In front of the coil ("Vac-0"), the e ± spectrum peaks at the nominal beam energy (10 GeV), as expected. In the CPR region ("Vac-3"), the spectrum peaks sharply at zero energy, and most e ± secondaries are below around 1 GeV, for 10 GeV incident. Figure (2a) shows the fraction of the initial 10 GeV electron energy carried by e ± secondaries in vacuum regions 1, 2, and 3; in the CPR region ("Vac-3"), the distribution of e ± fractional energy is approximately flat. Figure (2b) shows the complementary distributions of fractional energies carried by photons. (In Fig. (2), at each layer, there is one entry per 10 GeV shower, namely a sum over secondary e ± or photons in that layer). Figure (3) indicates how shower energy is propagated from the coil region to the CPR; it shows the CPR response as a function of the energy distribution of secondaries in the coil region. In Fig. (3), we define the CPR response to be the total dE/dx deposition in CPR by e ± secondaries; these have a mean dE/dx of 2.6 KeV, so that "CPR = 15" means 5.8 e ± secondaries in CPR, on average, each with 2.6 KeV dE/dx. The cutoff energy is used to reject secondaries in the coil region (the three regions with nonzero "B" in the EGS layout). The solid curve shows the effect of rejecting secondary e ± in the coil region, and the dashed the effect of rejecting secondary photons. For example, if we remove all secondary photons in the coil region (cutoff = 10,000 MeV for 10 GeV incident electron), then the CPR response is reduced from 15 to 5, about a factor of three. In general, if we remove low energy electrons (e.g., below 200 MeV) in the coil region, the effect on the CPR response is rather small; indeed most of the CPR response can be traced to high energy electrons and radiated photons in the coil region. This suggests that the CPR should be relatively insensitive to loss of soft e ± in the coil region due to B-field effects.

Figures 1-3 are for B = 0 in the coil region. Figure (4) shows the CPR response as a function of the B field, for 1, 2, and 10 GeV incident energies. It appears that B fields of order 1-2 T have no appreciable effect on CPR, and B-fields in excess of 10 T are needed to quench the CPR response. Needless to say, we would expect this conclusion to hold up for energies above 10 GeV as well.

3) "Massless Gap" CEM Energy Corrections

Since the B-field has no effect on the CPR response, we set B = 1.5 T in the "massless gap" analysis. Here we have considered three different configurations of radiators, in order to assess the effect of the 1/sin (θ) variation of radiator thickness, and also to see how these results would extrapolate to the SDC detector. The three configurations are:

A) Same as above, 1.1 X0 radiator in the CTC/CDT/Coil/Cryo system.

B) Doubled....., 2.2 X0 total radiator (e.g. sin (θ) = 0.5).

C) Doubled plus 0.6 additional X0 in front of CPR, 2.8 X0 total.

The CPR pulse height from EGS4 is basically just the product of the number of e ± secondaries in CPR times the average dE/dX in the 1 cm gap (2.6 KeV). To simulate the CPR more realistically, we have smeared each e ± secondary according to the dE/dx distribution observed for MIP's in CES; this is a Landau-like curve satisfying the relation

$$dE/dx\ (\text{Mean}) = dE/dx\ (\text{most probable})\ X\ 1.88.$$

Figures (5 a,b,c) show the CPR pulse height distributions for configurations A, B, and C, respectively. Figures (6 a,b,c) show the mean CPR response in KeV for these configurations, plotted as a function of the total energy deposited in the CEM (e.g. the total energy of secondary photons and electrons that exit the CPR). We did not actually simulate the CEM shower response, so albedo effects (shower energy back-scattered from CEM into CPR) could modify the CPR-CEM correlations slightly. We observe that, as the CEM energy is reduced from its maximum value (CEM/E0 =1.0), the CPR response increases; an eyeball fit gives:

$$[1.0 - CEM/E0] = CPR/\ C,$$

where

$$C = 900\ (A),\ 600\ (B),\ 400\ (C)\ \text{KeV}.$$

Thus, if the CPR resolution were perfect, we could correct the observed CEM energy to recover the true electron energy via:

$$CEM^*/E0 = CEM/E0 + CPR/C,$$

so that on average the corrected quantity, CEM*, satisfies

$$\langle CEM^*/E0 \rangle = 1.0$$

The quantity "C" above is some (nonlinear) function of energy, so such a correction would be made iteratively (estimate E0 from CEM, determine "C", then obtain CEM*). In practice, shower fluctuations are very large in the CPR pulse height (cf. Fig.(5)), so the above correction in general will not optimize the resolution on the CEM* energy. Instead we consider a weighted correction,

$$CEM^*/E0 = CEM/E0 + Weight * CPR/C.$$

The weight may be chosen to minimize the spread in CEM*/E0; note that the actual calibration of CEM*/E0 is irrelevant, since we are free to apply an overall scale factor to CEM or CEM* to specify the final calibration. Figure (7 a,b,c) shows the resolution on the corrected energy, as a function of the weight factor. In each case, there is a broad minimum with weights between 0.4 and 0.7. The weight = 1 case, which corrects "exactly" for the CPR-CEM correlation, gives poorer resolution because it allows the CPR fluctuations to become important; the weight = 0 case, which is free of CPR fluctuations, gives poorer resolution because it provides no correction for the fluctuations of energy loss in the coil material. In each configuration, optimal weighting improves the resolution by about 25%, compared with the weight = 0 case. The resolutions shown reflect only the fluctuations in the amount of shower energy entering the CEM. They do not reflect sampling fluctuations within CEM, which would be around 4.3% $\left(13.5\%/\sqrt{(E)}\right)$ at 10 GeV in the CDF detector. Thus, for the CDF configuration (Case A), the optimal resolution of 0.6% is much smaller than the sampling resolution. For Case B (2.2 X0), the massless gap correction would improve the overall resolution from 5.2% to 4.8% for 10 GeV electrons (e.g., adding the coil fluctuation resolution shown in Fig. (7 b) to the sampling resolution in quadrature). Case (B) corresponds to the SDC barrel calorimeter at $\eta = 1.3$. For Case (C) (2.2 X0 coil plus additional 0.6 X0 outside coil), the coil fluctuations are already worse than the 4.3% sampling resolution for 10 GeV electrons, so for this case the CPR correction is useful, and will improve the overall resolution by around 20%. Case (C) is roughly what a liquid argon SDC calorimeter would look like at $\eta = 1.3$. Finally, Figures (8 a,b,c) show the CEM/E0 distributions for unweighted (bottom) and optimally weighted (top) cases for configurations A,B, and C respectively. The resolution improvement is clear in each case, but again these distributions show only the loss fluctuations due to the coil, and do not include the (larger) CEM sampling fluctuations.

For completeness, we have examined the energy dependence of the coil loss fluctuations. We consider case (B) only, since the effects are negligible in case (A). We have repeated the EGS studies for case (B) at 2, 10, 50, and 100 GeV. Figure (9) shows the average and RMS values of the CPR pulse height distribution versus energy. The CPR response is nonlinear, and the RMS width, expressed as $\sigma(CPR)/\langle CPR\rangle$, is roughly constant with energy (does not fall as $1\sqrt{E}$). The actual fraction of electron energy lost before the calorimeter is shown in Fig. (10). This loss fraction falls rapidly with energy, roughly mimicking the energy dependence of the $\langle CPR\rangle$ response. Figure (11) shows the ratio of coil loss fluctuation to stochastic resolution, where for concreteness we have assumed a stochastic resolution of $15\%/\sqrt{E}$. This ratio is plotted for the raw calorimeter energy with no CPR correction (top curve) and optimal CPR correction (bottom curve). Adding

the coil fluctuations and the stochastic resolutions in quadrature, we see that the overall resolution is degraded by amounts ranging from 30% at 2 GeV to 11% at 100 GeV, with no CPR weighting. Using optimal CPR weighting improves the overall resolution (i.e., stochastic plus coil loss fluctuations added in quadrature) by less than 10% over this energy range, as compared with the unweighted case. We can conclude that (1) the resolution degradation caused by coil losses falls with energy, relative to the stochastic term, because the coil loss fraction itself falls with energy; (2) the CPR weighting correction gives rather modest improvements in the overall (stochastic plus coil loss) resolution, presumably because the intrinsic fluctuations in the CPR response are large (of order 50%) at all energies.

4) Conclusions

We conclude that B-field effects are negligible in the CPR pulse height response. This is because the low energy secondaries that would be quenched by the B-field do not contribute significantly to the CPR response (they are ranged out in the coil material). We also conclude that "massless gap" corrections might be important for large angles, but are irrelevant in the CDF central region, where the coil material is close to 1.1 X0; the resolution improvement offered by a massless gap correction would be negligible compared with the CEM sampling resolution for energies of interest. For the SDC at large η, the coil loss fluctuations become significant, but the massless gap corrections offer improvements of less than 10% in the overall calorimeter resolution.

Figure Captions

1) Energy spectra of secondary e ± at the four "vacuum" layers.

2) Fraction of initial electron energy carried by (a) e ±,
(b) photons, in the "vacuum" layers 1, 2, and 3.

3) Average CPR pulse height as a function of the cutoff energy applied to secondaries (solid = e ±, dashed = photons) in the nonzero-B field region.

4) Average CPR pulse height versus B-field for 1, 2, and 10 GeV incident electrons.

5) CPR pulse height distribution for the three radiator configurations, A, B, and C.

6) Average CPR energy as a function of the CEM/E0 energy fraction, for configurations A, B, and C.

7) RMS spread in CEM/E0, as a function of the weight used for CPR correction, for configurations A, B, and C. Sampling fluctuations in CEM are not included.

8) Distributions in CEM/E0 for zero weight and optimal weight, for configurations A, B, and C. CEM sampling fluctuations are not simulated.

9) CPR average response and RMS width versus energy, normalized to incident energy (KeV per GeV) for case (B) (2.2 X0). The dashed curve shows the fractional resolution, $\sigma(CPR)/\langle CPR\rangle$, obtained by dividing the two solid curves.

10) Average fractional loss in coil system, for case (B) (2.2 X0) versus energy.

11) Ratio of coil fluctuation to stochastic resolution, assuming $15\%/\sqrt{E}$ for the latter, versus energy; with no CPR weighting (W = 0 curve), and with optimal CPR weighting at each energy (W = optimal curve). Case (B) (2.2 X0) is shown.

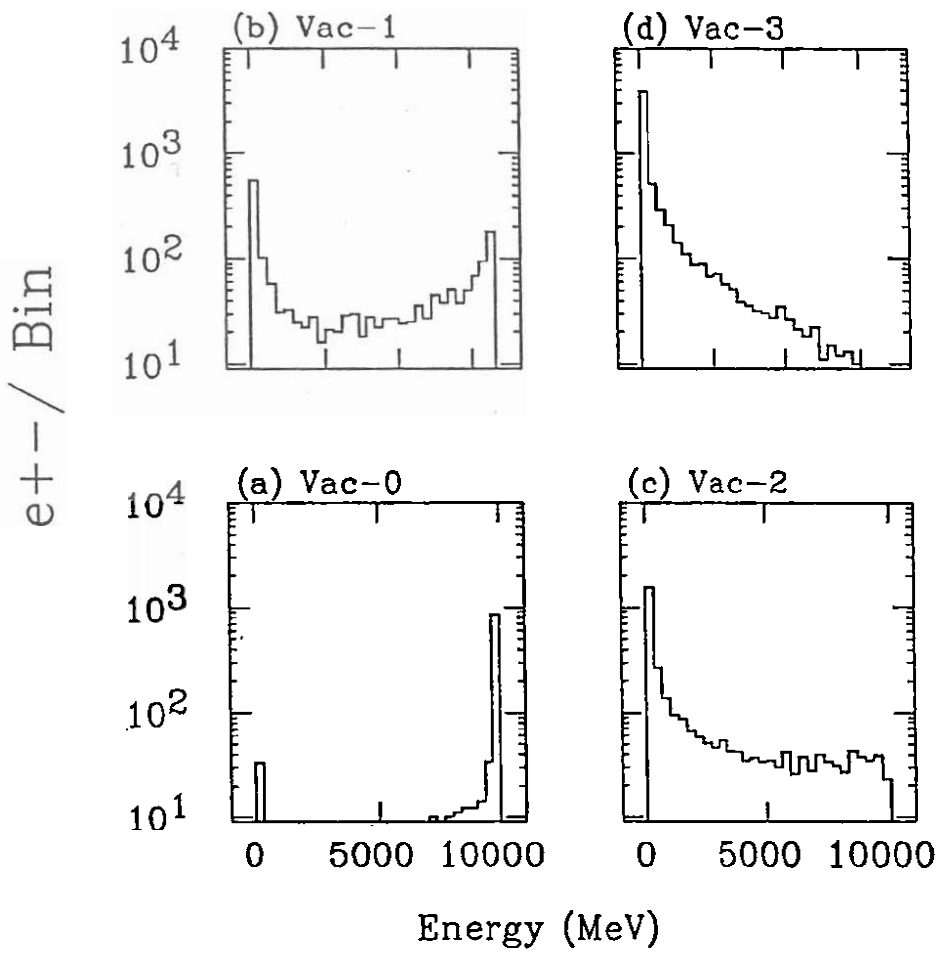
(b) Vac−1
(d) Vac−3
(a) Vac−0
(c) Vac−2
10^4
10^3
10^2
10^1
e+−/ Bin
0
5000
10000
Energy (MeV)

Figure 1

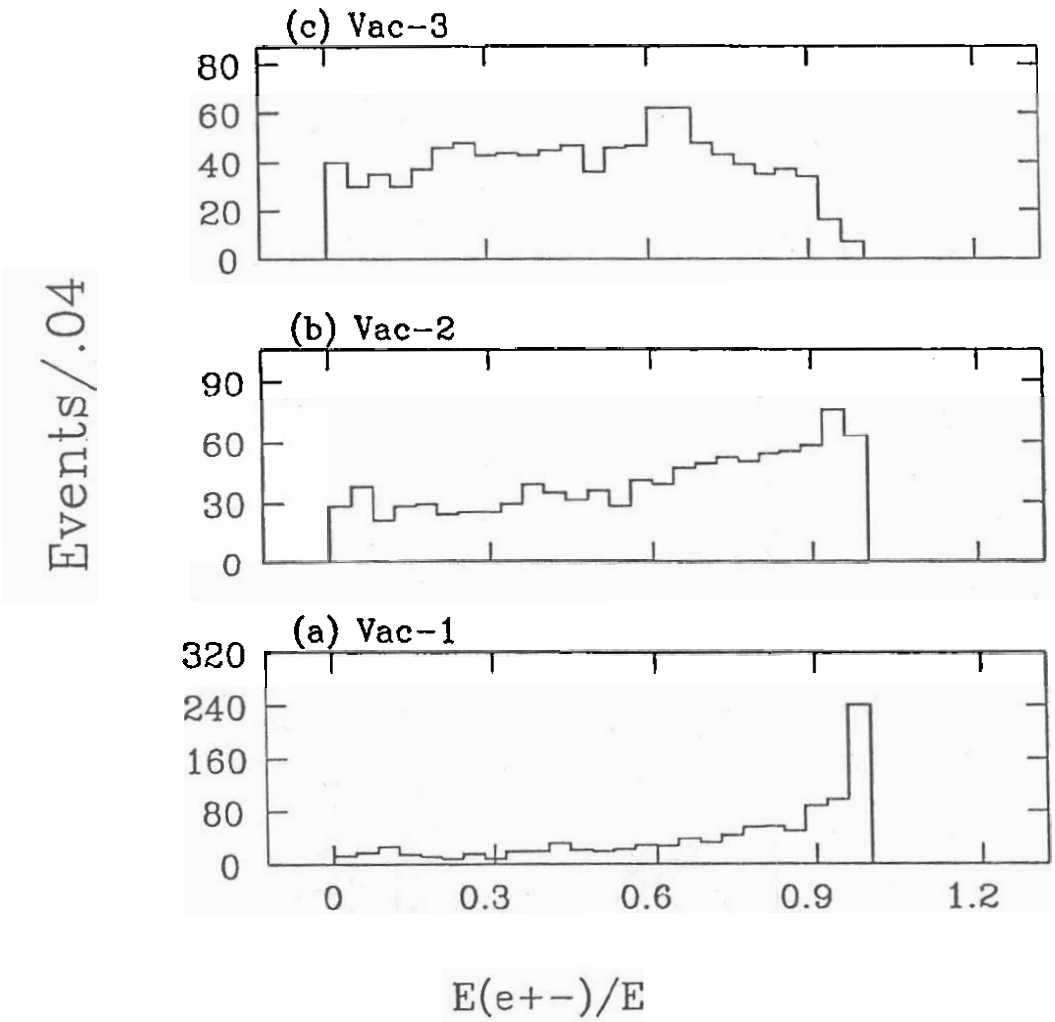
(c) Vac-3
80
60
40
20
0
(b) Vac-2
90
60
30
0
(a) Vac-1
320
240
160
80
0
0
0.3
0.6
0.9
1.2
Events/.04
E(e+-)/E

Figure 2a

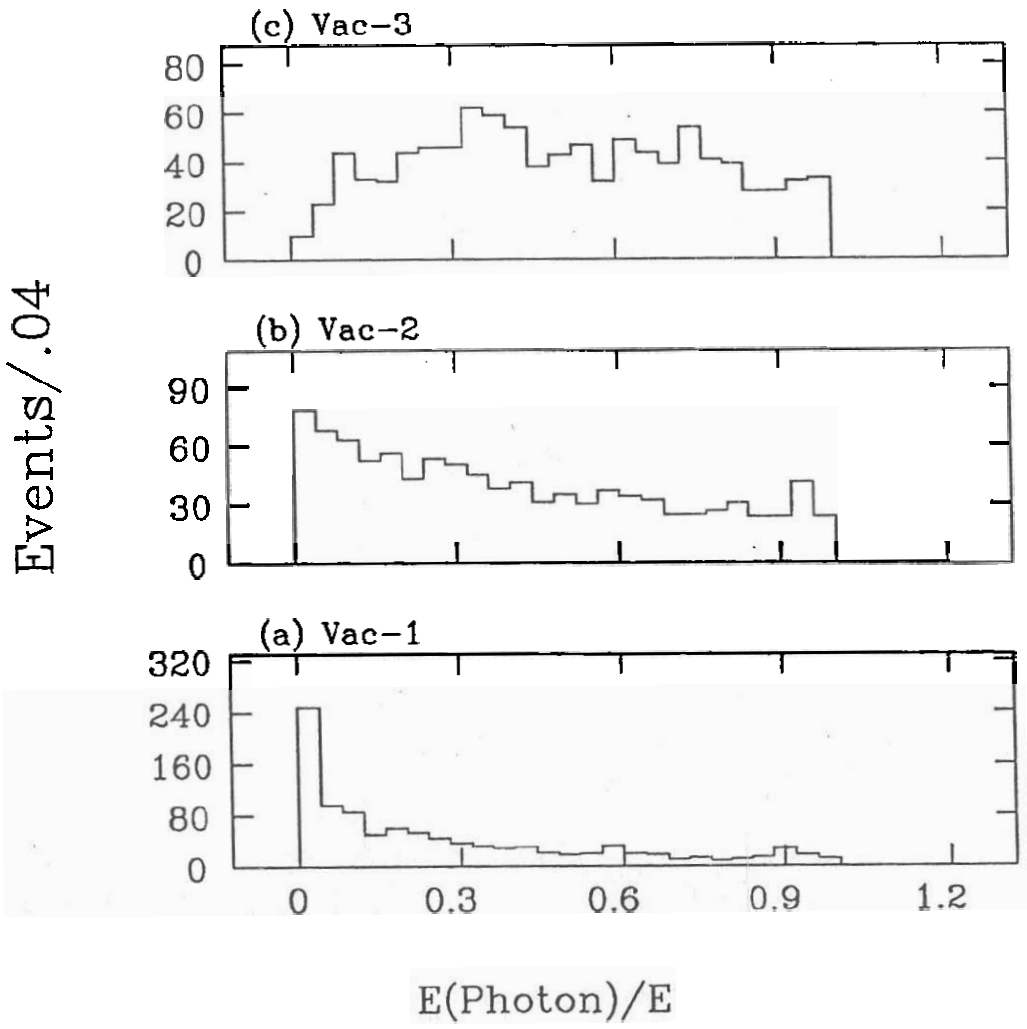
(c) Vac−3
80
60
40
20
0
(b) Vac−2
90
60
30
0
(a) Vac−1
320
240
160
80
0
0
0.3
0.6
0.9
1.2
Events/.04
E(Photon)/E

Figure 2b

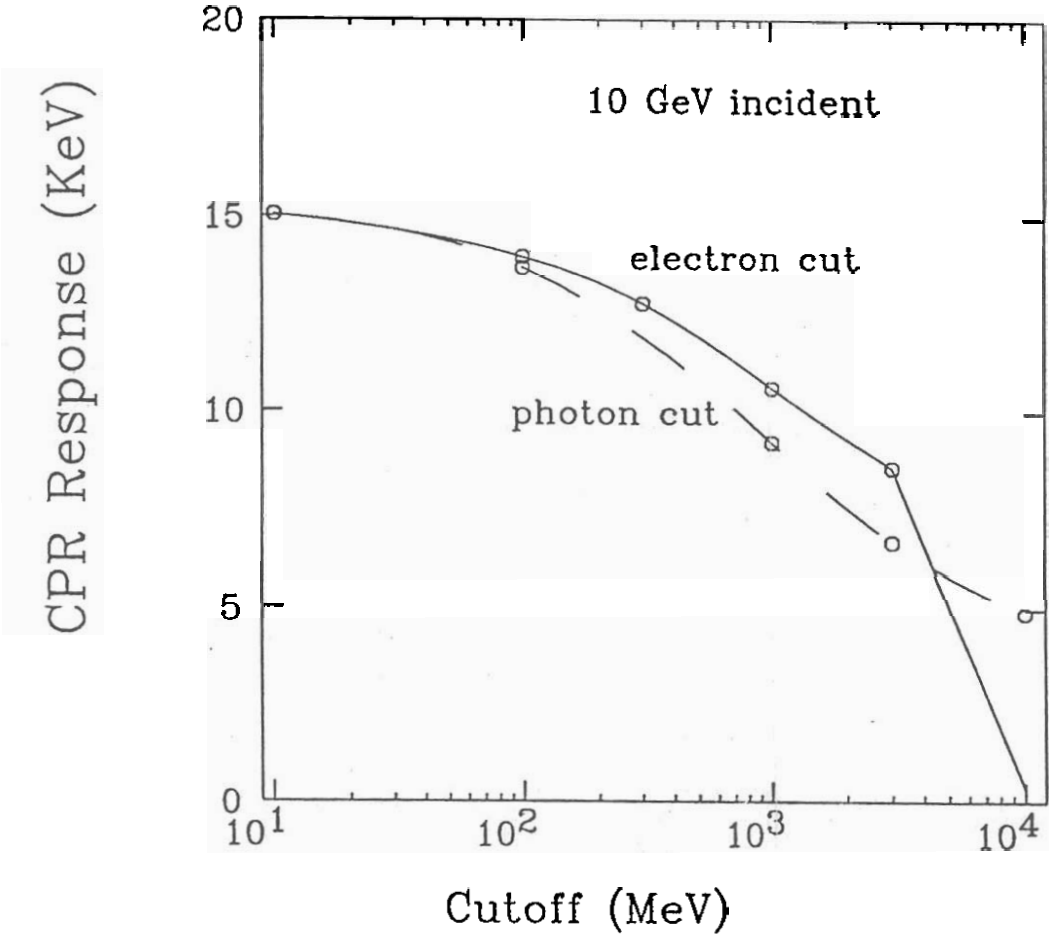
20
15
10
5
0
10 GeV incident
electron cut
photon cut
CPR Response (KeV)
10^1
10^2
10^3
10^4
Cutoff (MeV)

Figure 3

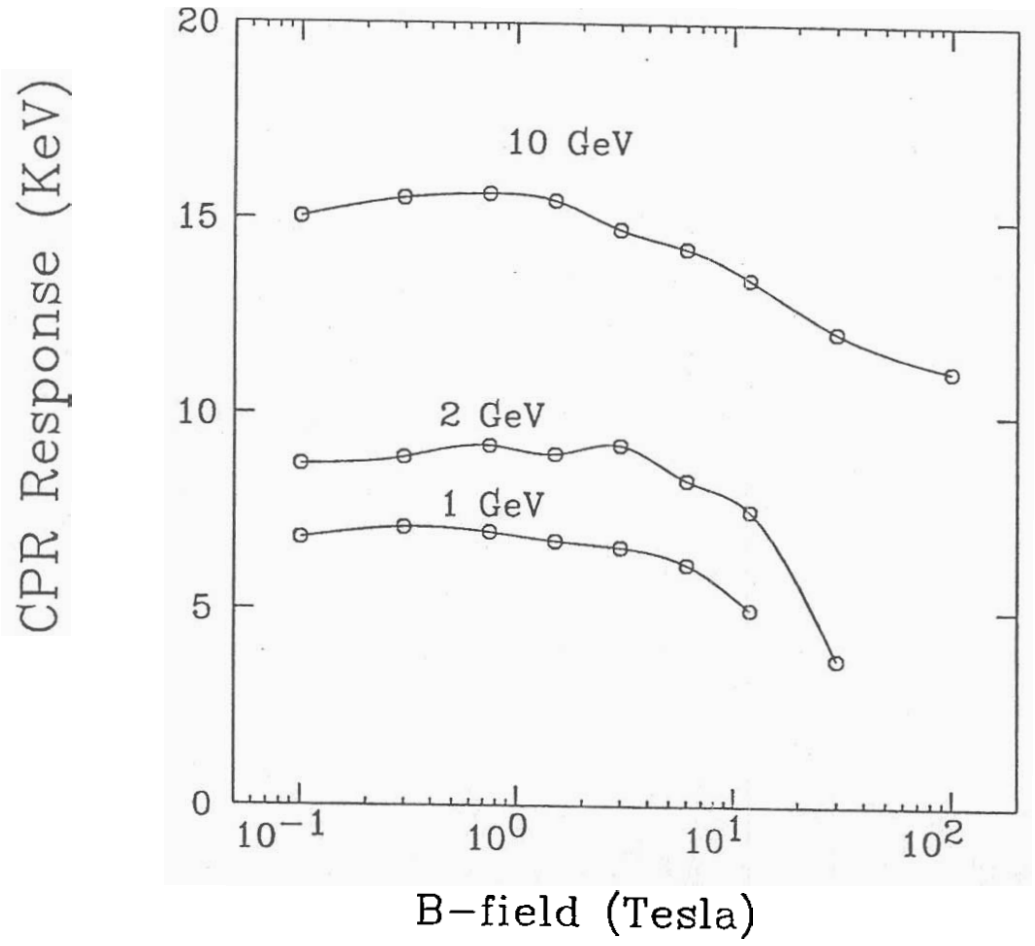
CPR Response (KeV)
20
15
10
5
0
10 GeV
2 GeV
1 GeV
10^{-1}
10^{0}
10^{1}
10^{2}
B−field (Tesla)

Figure 4

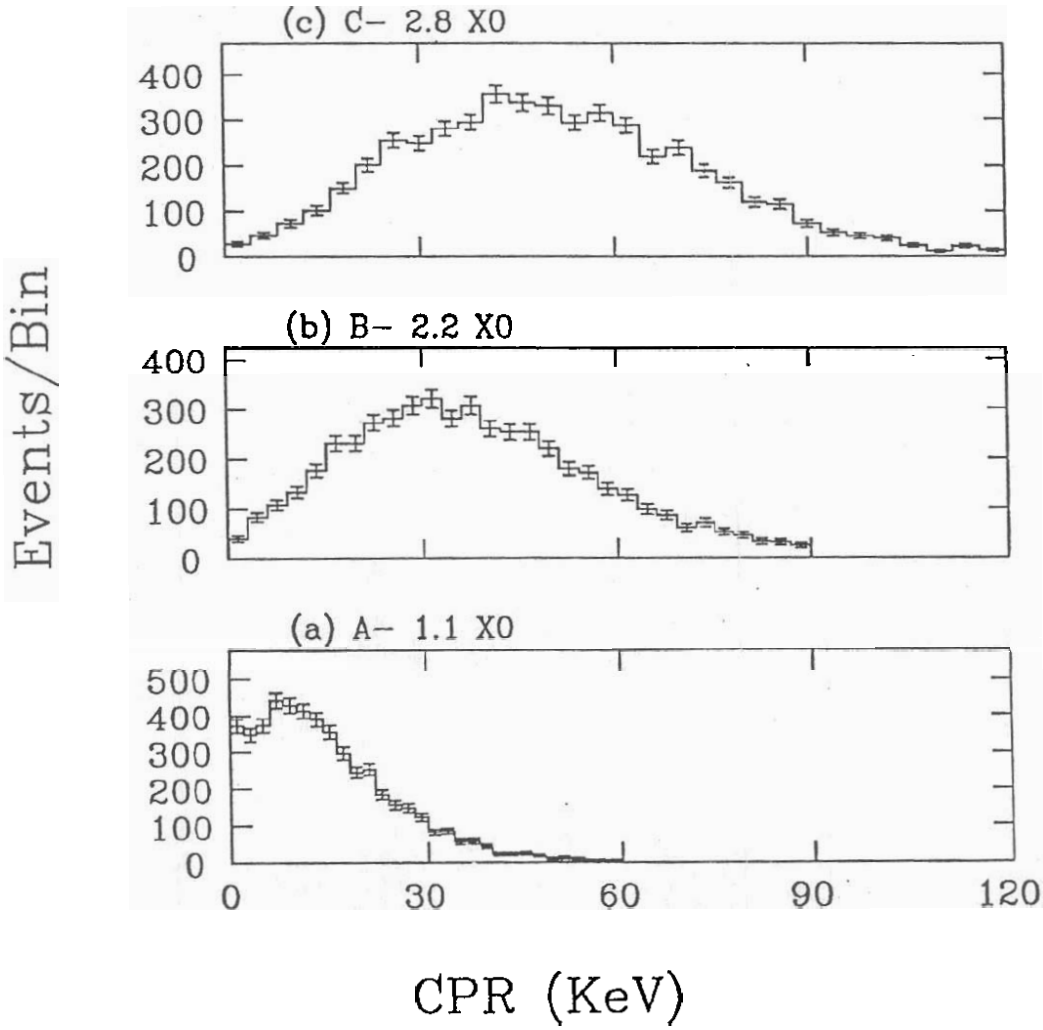
(c) C– 2.8 X0
(b) B– 2.2 X0
(a) A– 1.1 X0
Events/Bin
400
300
200
100
0
500
0
30
60
90
120
CPR (KeV)

Figure 5

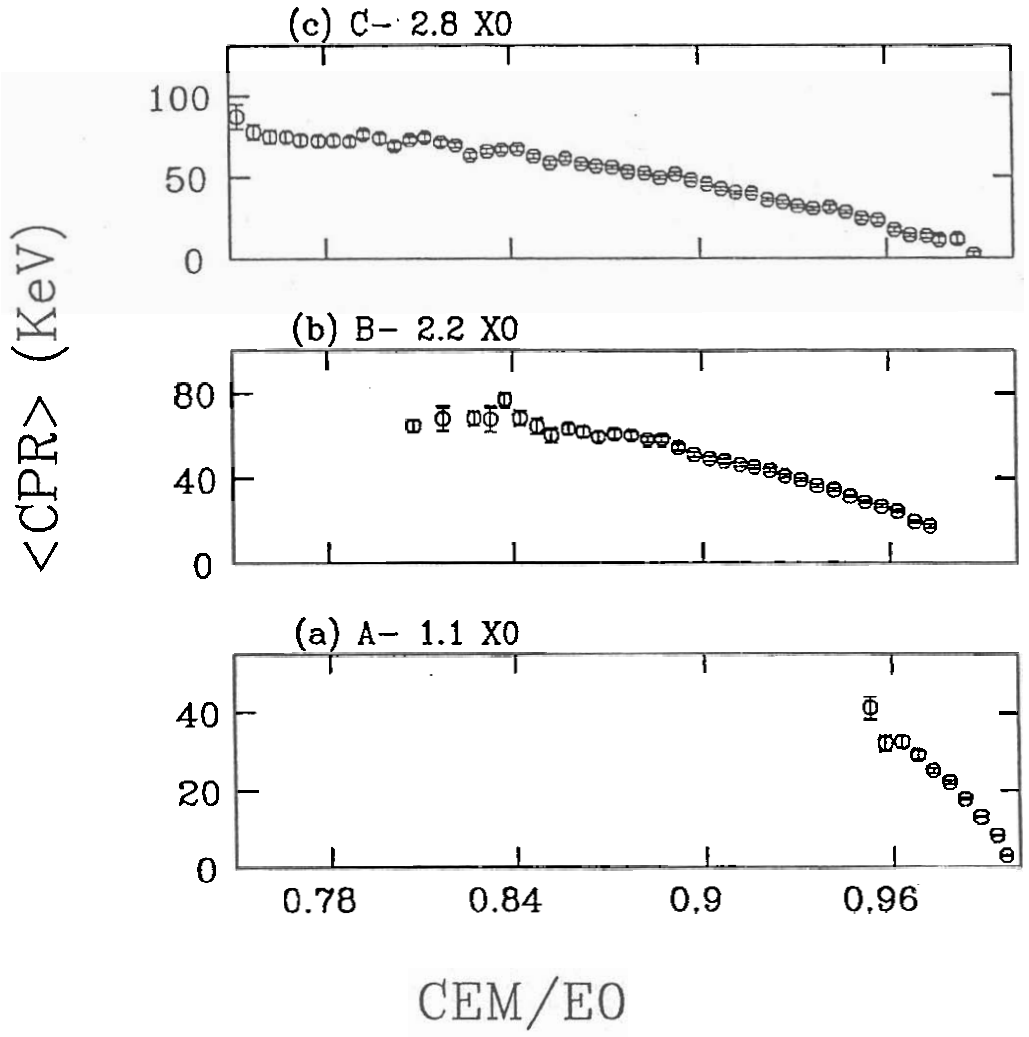
(c) C- 2.8 X0
100
50
0
(b) B- 2.2 X0
80
40
0
(a) A- 1.1 X0
40
20
0
0.78
0.84
0.9
0.96
<CPR> (KeV)
CEM/E0

Figure 6

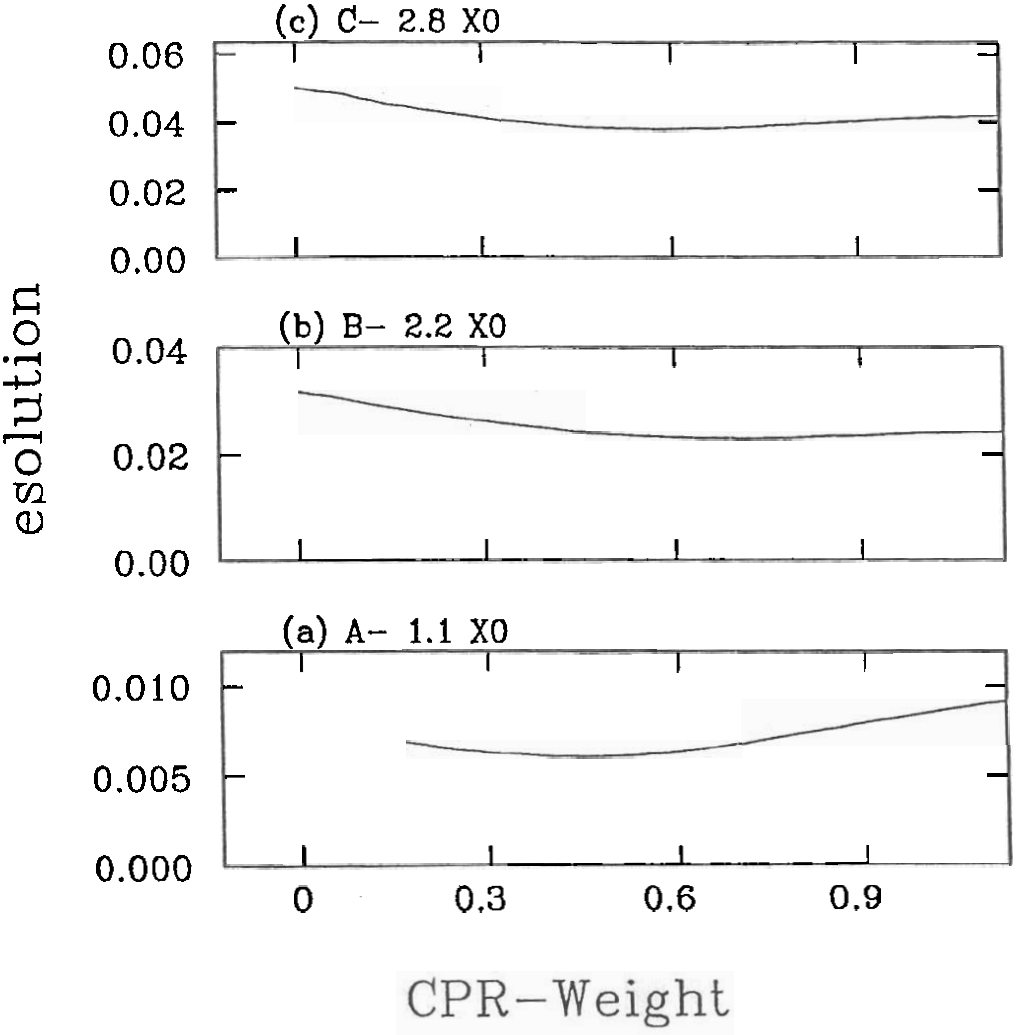
(c) C- 2.8 X0
0.06
0.04
0.02
0.00
(b) B- 2.2 X0
0.04
0.02
0.00
(a) A- 1.1 X0
0.010
0.005
0.000
0
0.3
0.6
0.9
esolution
CPR-Weight

Figure 7

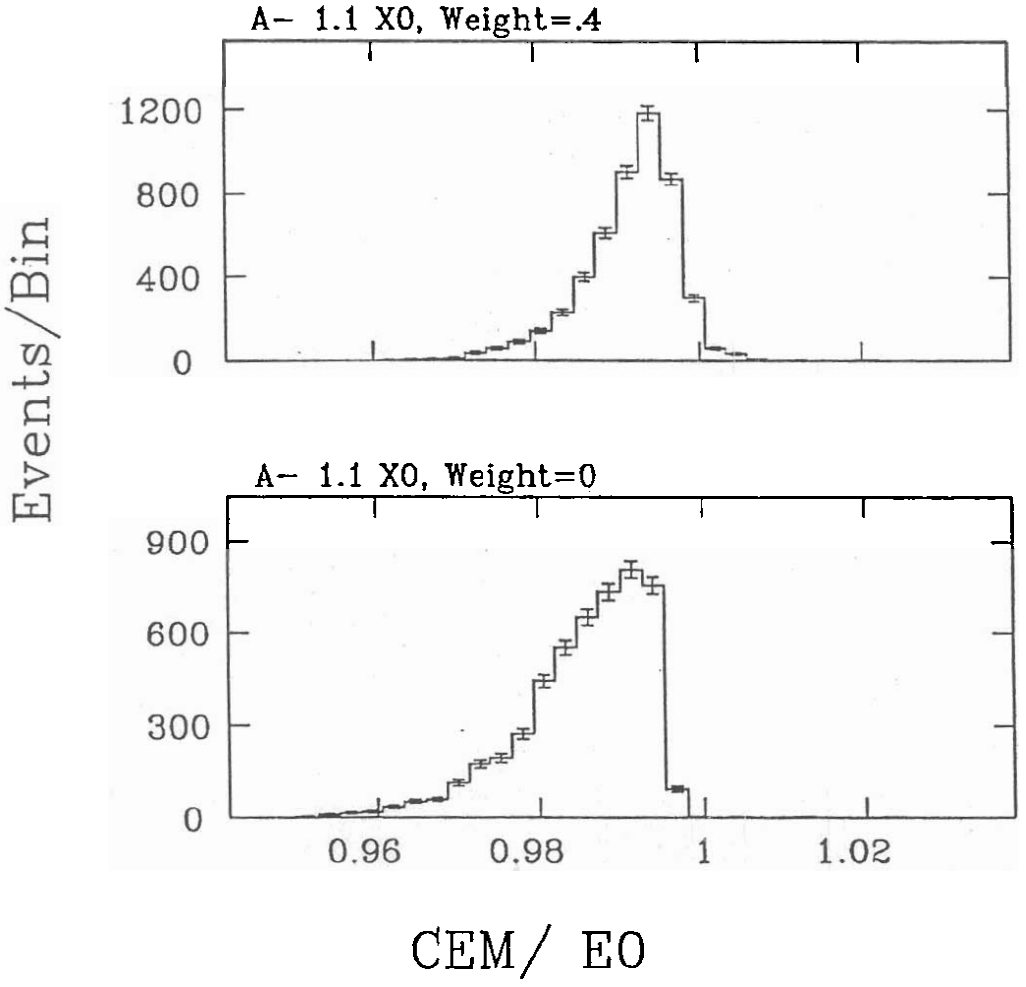
A- 1.1 X0, Weight=.4
1200
800
400
0
Events/Bin
A- 1.1 X0, Weight=0
900
600
300
0
0.96
0.98
1
1.02
CEM/ E0

Figure 8a

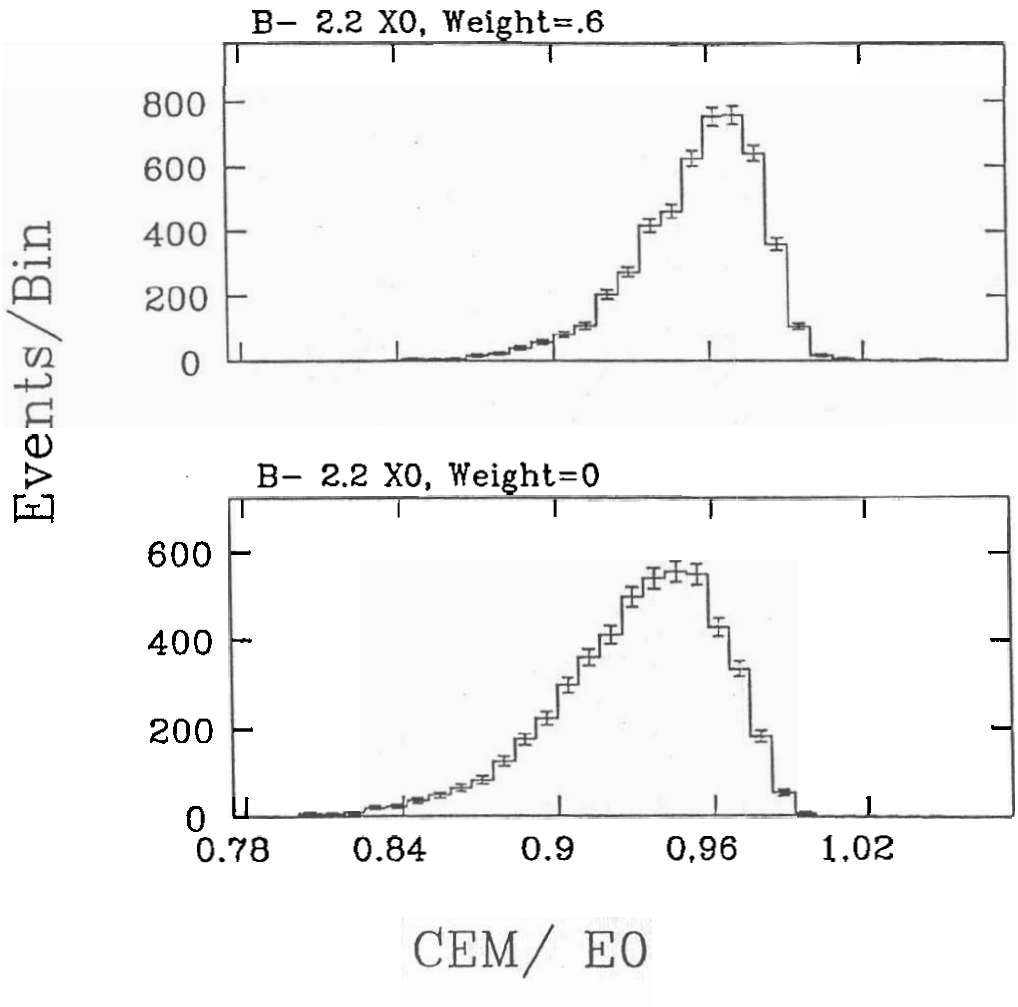
B- 2.2 X0, Weight=.6
800
600
400
200
0
Events/Bin
B- 2.2 X0, Weight=0
600
400
200
0
0.78
0.84
0.9
0.96
1.02
CEM/ E0

Figure 8b

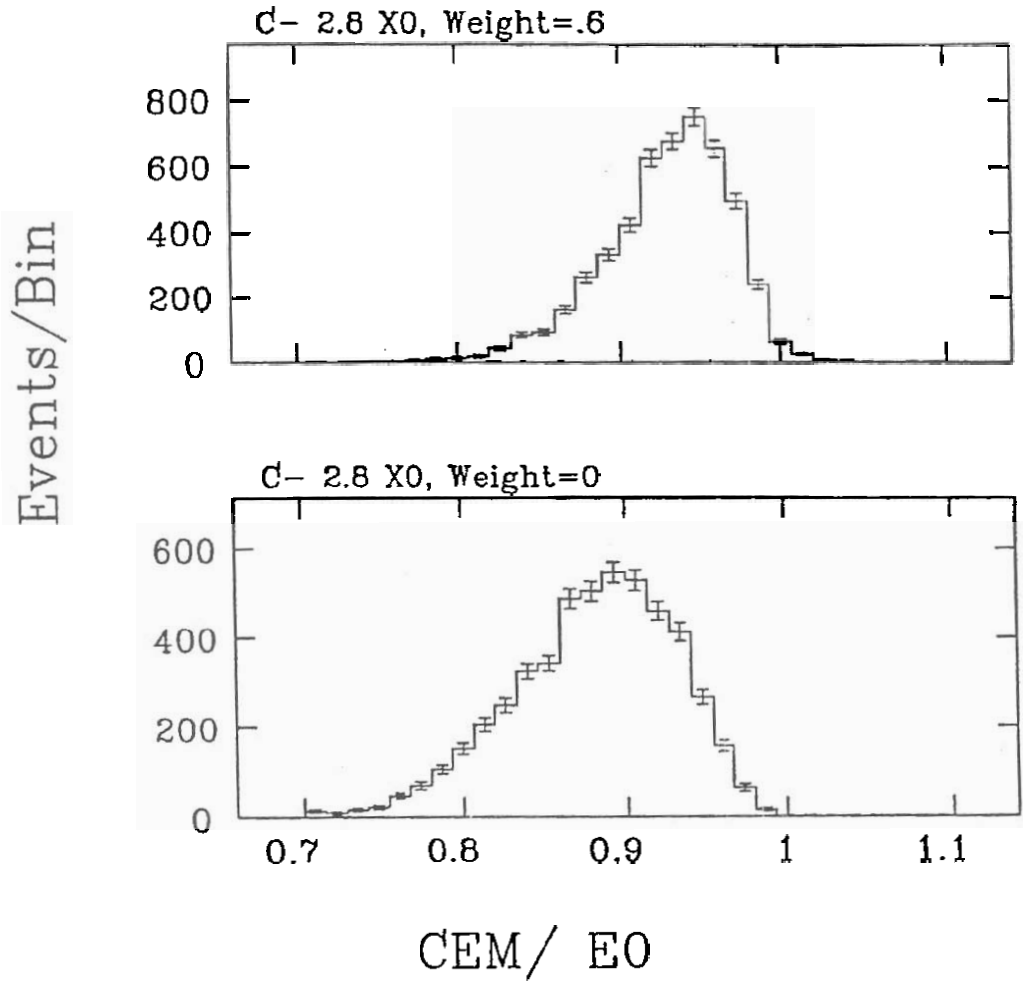
C- 2.8 X0, Weight=.6
800
600
400
200
0
Events/Bin
C- 2.8 X0, Weight=0
600
400
200
0
0.7
0.8
0.9
1
1.1
CEM/ E0

Figure 8c

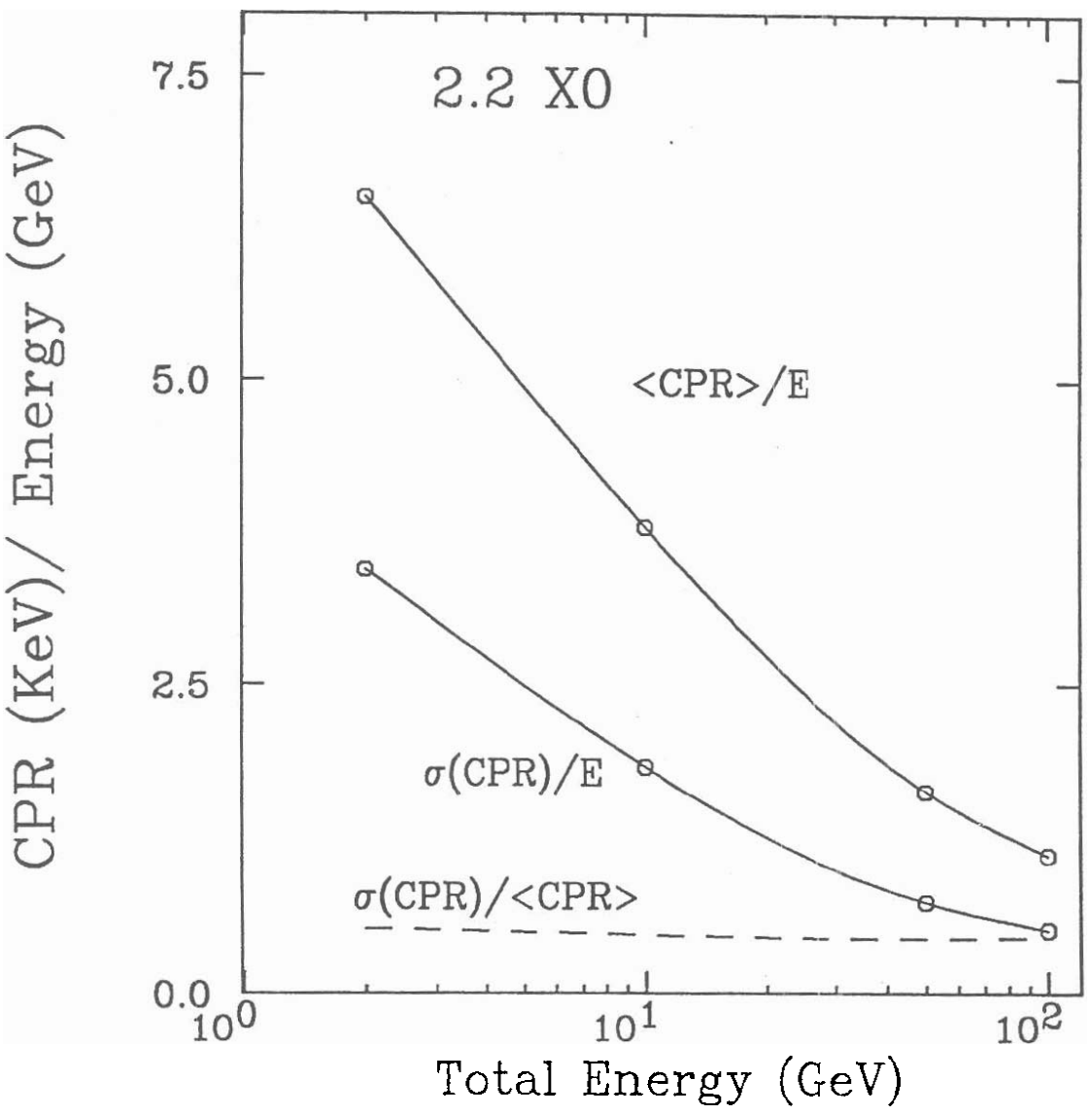
2.2 X0
7.5
5.0
2.5
0.0
<CPR>/E
σ(CPR)/E
σ(CPR)/<CPR>
CPR (KeV)/ Energy (GeV)
10^0
10^1
10^2
Total Energy (GeV)

Figure 9

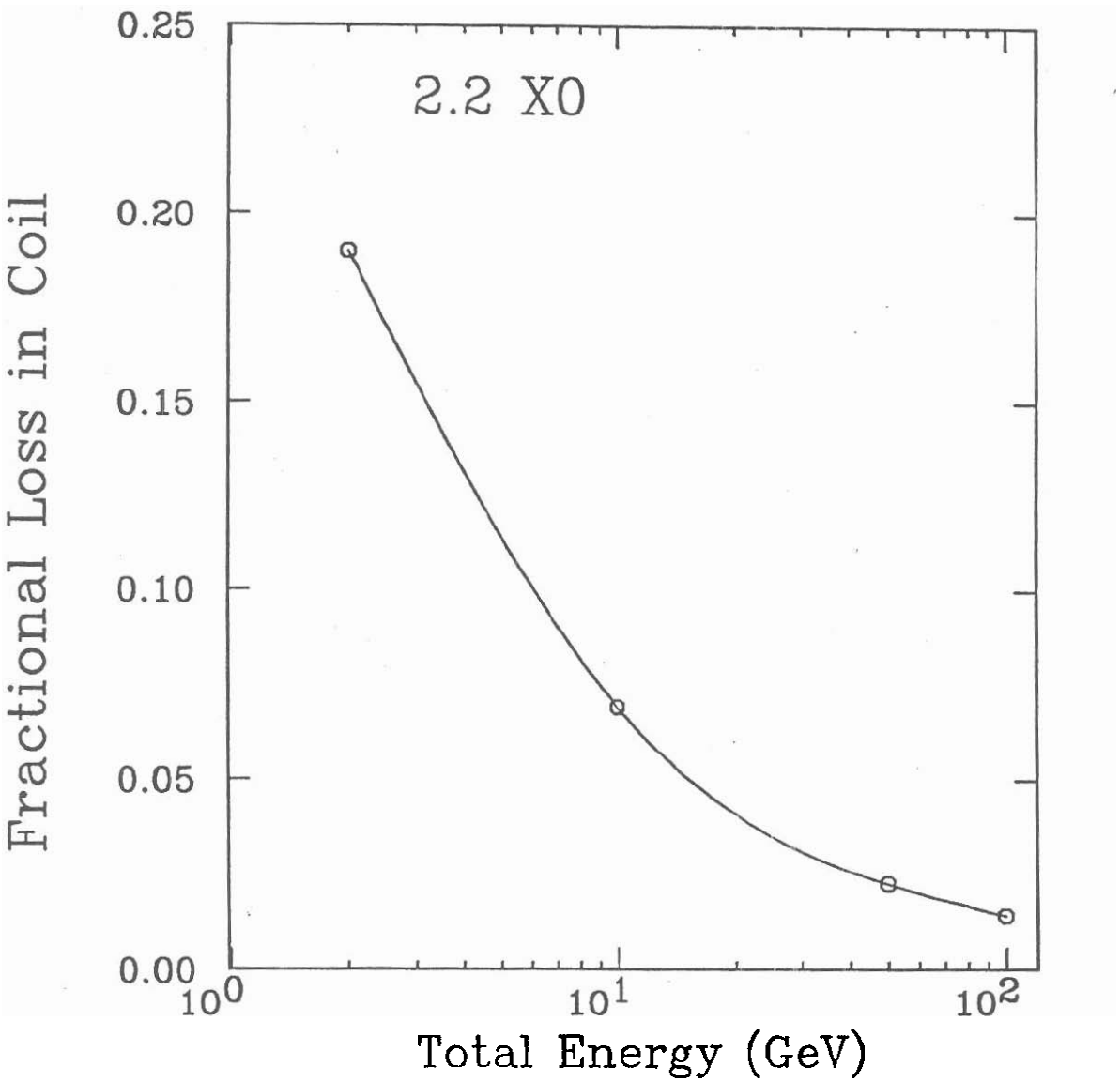
2.2 X0
Fractional Loss in Coil
0.25
0.20
0.15
0.10
0.05
0.00
10^0
10^1
10^2
Total Energy (GeV)

Figure (10)

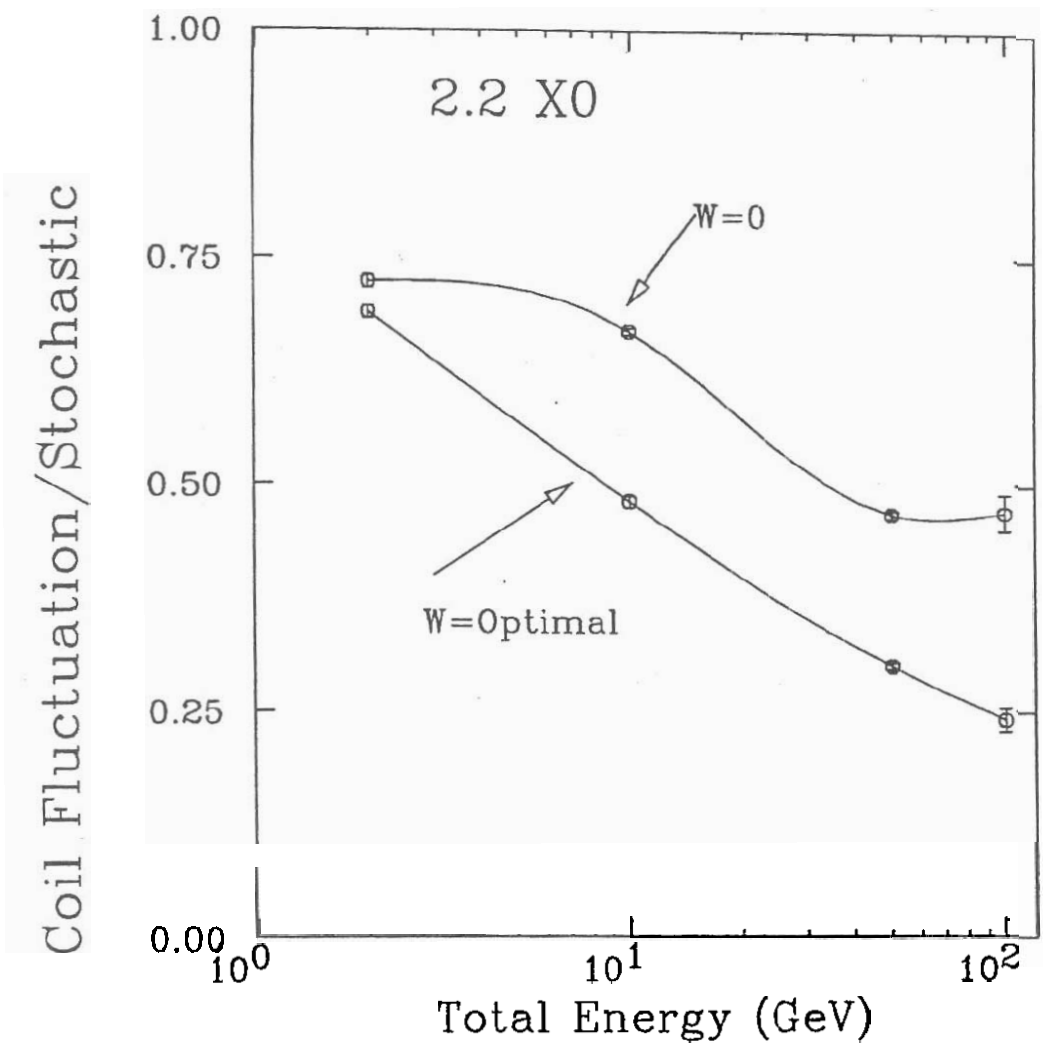
2.2 X0
W=0
W=Optimal
1.00
0.75
0.50
0.25
0.00
10^0
10^1
10^2
Coil Fluctuation/Stochastic
Total Energy (GeV)

Figure 11